remote sensing

MDPI

Article

Spatial-Temporal Evolution of Proglacial Lake Volumes and Estimation Models in the Himalaya and Nyainqentanglha Ranges

Miaohui Zhang [1,2], Hao Wang [3,*], Peng Cui [1], Jinbo Tang [3], Yilong Yu [2,3], Jingxuan Cao [2,3], Xuan Liu [3], Jingxi Yang [4], Yunpeng Liu [4] and Qingchun Li [4]

1 Institute of Geographic Sciences and Natural Resources Research, Chinese Academy of Sciences, Beijing 100101, China
2 University of Chinese Academy of Sciences, Beijing 100049, China
3 Institute of Mountain Hazards and Environment, Chinese Academy of Sciences, Chengdu 610041, China
4 POWERCHINA Chengdu Engineering Corporation Limited, Chengdu 611130, China
* Correspondence: hwang@imde.ac.cn

Highlights

What are the main findings?

- We developed optimized regional empirical models by integrating field-based bathymetric surveys of 10 proglacial lakes, showing superior performance in volume and depth estimation compared to 14 established global formulas.
- Spatiotemporal reconstruction reveals a significant and heterogeneous expansion from 1990 to 2020, with lake volumes in the Nyainqentanglha range increasing by 92.9% over the past three decades.

What is the implication of the main finding?

- These refined scaling relationships offer critical parametric constraints for satellite-based monitoring, substantially improving the accuracy of GLOF hazard assessments and peak discharge estimations across the Himalaya and Nyainqentanglha Range.

Abstract

Volume quantification of proglacial lakes is a fundamental prerequisite for reliable hydrodynamic modeling and peak discharge estimation during glacial lake outburst floods (GLOFs). In this study, we integrated in situ bathymetric surveys of 10 proglacial lakes across the Himalaya and Nyainqentanglha ranges with a comprehensive regional dataset to derive optimized empirical models for lake volume and maximum depth. The predictive robustness of these models was rigorously validated using statistical error metrics and independent datasets. Comparative analysis with 14 established formulas demonstrates that our region-specific models yield superior performance in capturing local geomorphological characteristics. Leveraging these refined scaling relationships, we reconstructed the spatiotemporal volume changes in proglacial lakes across the study region from 1990 to 2020. Our analysis reveals significant lake expansion over the past three decades: lake volumes in the Western and Central Himalayas increased by 46.7% and 46.4%, respectively. Notably, the Eastern Himalayas exhibited a volume increase of 51.5%, while the Nyainqentanglha Mountains experienced a substantial expansion of approximately 92.9%. These findings provide critical parametric constraints for satellite-based hydrological monitoring and significantly enhance the reliability of GLOF hazard assessments in the Himalaya and Nyainqentanglha ranges.

Academic Editor: Pavel Kishcha

Received: 2 March 2026
Revised: 5 May 2026
Accepted: 25 May 2026
Published: 7 July 2026

Keywords: proglacial lakes; bathymetry; empirical models; remote sensing; Himalaya; Nyainqentanglha

1. Introduction

Climate warming has driven a global glacier mass loss rate of 273 ± 16 Gt yr^{-1} during the period 2000–2023. Relative to the 2000–2011 baseline, the average annual mass loss from 2012 to 2023 increased by 36% ± 10%, underscoring an accelerating trend in glacier ablation [1]. From 1980 to 2018, the Asian Water Tower (AWT) exhibited a warming rate of 0.42 °C per decade, approximately double the global average [2,3]. Global warming has induced a negative mass balance and continuous retreat of glaciers in the AWT region, leading to a cumulative mass loss of 340 Gt and triggering the rapid expansion of glacial lakes. Over recent decades, mountain glacial lakes across High Mountain Asia (HMA) have experienced significant expansion in surface area and drastic fluctuations in water storage, with long-term hydrological evolution patterns exhibiting distinct regional differentiation [4].

Glacial lakes are typically defined as natural impoundments originating from meltwater derived from contemporary glaciers or situated within glacial terminal moraines. Taxonomically, they are categorized based on their spatial proximity to the glacier terminus into proglacial, supraglacial, and subglacial lakes [5]. As critical freshwater reservoirs in the high-mountain cryosphere, glacial lakes demonstrate high sensitivity to climate change [6]. Between 1990 and 2018, the number, surface area, and volume of glacial lakes globally increased by 53%, 51%, and 48%, respectively [7]. Notably, proglacial lakes expanded at a markedly higher rate compared to other categories. Between 2018 and 2022, proglacial lakes comprised 83% of the total areal expansion of glacial lakes [8]. Moreover, lake-terminating glaciers typically undergo more severe negative mass balances than their land-terminating counterparts. Thermal convection in proglacial lakes intensifies subaqueous ablation and calving, thereby driving lake expansion [9–11]. By the end of this century, cryospheric degradation across the Third Pole is projected to significantly amplify the total water volume of proglacial lakes on the Qinghai–Tibet Plateau [12]. This acceleration is driven by warming-induced calving and subaqueous melting, which create a positive feedback amplifying lake expansion [13].

Terminal moraine dams of proglacial lakes typically comprise coarsely graded glacial till characterized by poor sorting and reduced geotechnical stability [14]. External triggers, such as mass movements, such as ice/rock avalanches, or extreme precipitation, can destabilize these moraine dams, leading to catastrophic breaches [15–18]. Glacial lake outburst floods (GLOFs) are characterized by exceptionally high peak discharges and hydraulic impacts that significantly exceed those of seasonal monsoon floods, thereby exerting profound geomorphic influence and catastrophic destructive capability. These events significantly reshape the downstream channel morphology and cause severe damage to critical infrastructure, including bridges, highways, and hydropower facilities [19,20]. Global assessments indicate that GLOFs expose approximately 15 million people to potential risk [21]. Downstream communities have suffered substantial socioeconomic losses and fatalities attributable to these hazardous events. For instance, on 5 July 2016, the Gongbatongsha GLOF devastated downstream infrastructure, including the Araniko Highway and the Upper Bhotekoshi Hydropower Station, causing an estimated economic loss of $70 million [22]. Similarly, on 3 October 2023, a GLOF at South Lhonak Lake in Sikkim, India, caused 55 fatalities and 74 missing individuals, with over 25,900 buildings inundated and 31 major bridges destroyed [15]. Sustained glacial recession and lake expansion are expected to amplify the frequency of GLOFs. In the High Mountain Asia region, GLOF risk exposure is projected to triple by 2100 [17].

Hydrodynamic numerical models are widely used to quantify the magnitude of GLOFs and assess their downstream consequences [15,23–26]. However, the reliability of these assessments is constrained by the precision of the input data. In this context, the volume of glacial lakes constitutes a governing parameter in GLOF simulations [19]. It directly affects major hydraulic outputs, specifically total flood volume and peak discharge [15,26–28]. Consequently, underestimating lake volume during risk characterization may yield erroneous predictions of flood magnitude, potentially obscuring the true severity of the GLOF [29,30].

The most accurate approach for quantifying glacial lake volume remains in situ bathymetric surveys utilizing platforms such as unmanned surface vehicles (USVs) [27,31,32]. However, the inaccessibility and harsh climatic conditions characterizing the high-altitude environments of the Himalaya and Nyainqentanglha ranges render extensive field campaigns logistically prohibitive. Consequently, high-resolution bathymetric datasets for most proglacial lakes remain sparse. To address this data gap, various methodologies have utilized satellite remote sensing to derive bathymetry for large glacial lakes [33–35]. In complex alpine terrains, the acquisition of satellite-derived bathymetry is severely hindered by environmental constraints, notably persistent cloud cover, seasonal ice formation, and high turbidity. Furthermore, the attenuation of electromagnetic signals within the water column fundamentally limits the penetration depth and vertical accuracy required for precise subaqueous topographic mapping [36–38]. Given these limitations, empirical area-volume scaling relationships are widely adopted to approximate glacial lake volumes [31,39–52]. Nevertheless, conventional empirical formulas are predominantly derived from datasets originating in the Alps or Andes, which introduces geographical bias and constrains their transferability to other cryospheric regions [30,45,53,54]. Moreover, available in situ bathymetric data in the Himalayas are spatially biased toward the central region, precluding a representative characterization of proglacial lakes across the broader Himalaya and Nyainqentanglha ranges [24,31].

Accelerated global warming has intensified the retreat of parent glaciers, resulting in significant expansion of proglacial lake surface areas and modifications to basin bathymetry. These dynamic changes undermine the applicability of static empirical formulas derived from historical data [55,56]. Consequently, contemporary in situ measurements are imperative for validating, calibrating, and refining volume estimation models, thereby enhancing the precision of water storage capacity assessments for proglacial lakes in the Himalaya and Nyainqentanglha ranges [7,57]. Although growing attention has been devoted to glacial lake areal dynamics, long-term quantitative understanding of changes in lake volume across the study region from 1990 to 2020 remains limited, while the driving mechanism linking multi-decadal lake water storage variation to regional climate change still lacks targeted quantitative investigation. This study collates new field observations and existing literature to construct a comprehensive bathymetric database, mitigating the scarcity of observed depth data in these regions. The dataset encompasses bathymetric data for 79 proglacial lakes, comprising 10 newly surveyed lakes across the Central Himalaya, Eastern Himalaya, and Nyainqentanglha, supplemented by 69 records compiled from existing studies. Using this integrated dataset, the study investigates new relationships among key geomorphological parameters of the lakes. The objectives are threefold: (1) to expand the observational database of proglacial lake bathymetry across the Himalaya and Nyainqentanglha; (2) to derive regional empirical formulas for estimating lake volume and maximum water depth, quantitatively characterizing the scaling relationships among volume, depth, and area; and (3) to systematically evaluate the accuracy and uncertainty of the proposed models against prevailing established equations. The empirical framework presented here provides critical parametric constraints for GLOF hazard assessment in the Himalaya and Nyainqentanglha region.

2. Study Area

Situated along the southern edge of the Qinghai–Tibet Plateau, the study region comprises the Himalaya and Nyainqentanglha Ranges (72°46′39″E–97°52′53″E, 26°39′32″N–35°51′8″N), covering a total area of approximately 791,000 km^2 (Figure 1a). This region is physiographically subdivided into four distinct sectors: the Eastern Himalaya (166,000 km^2), Central Himalaya (256,000 km^2), Western Himalaya (194,000 km^2), and the Nyainqentanglha Mountains (175,000 km^2) (Figure 1b). The topography is characterized by extreme vertical relief, with local elevation gradients ranging from 6000 to 7000 m. Notably, 10 of the 14 peaks worldwide that exceed 8000 m are located in the Himalayas [58]. The Indian Summer Monsoon serves as the dominant moisture source for the southern Himalayas and the eastern Nyainqentanglha Mountains. In contrast, the northern and western flanks are governed by continental cold high-pressure systems and westerly interactions, resulting in predominantly arid conditions and a scarcity of precipitation [59]. Moreover, precipitation exhibits a pronounced longitudinal gradient, decreasing from east to west, with the southern slopes receiving approximately 6 to 7 times more precipitation than the northern slopes [60,61]. Despite a general trend towards increased wetness across the Qinghai–Tibet Plateau, substantial regional and seasonal variability persists [62]. In addition, the region demonstrates prominent Elevation-Dependent Warming [63,64], with a warming rate of approximately 0.5 °C per decade at elevations exceeding 4000 m [65]. The study area is characterized by intense neotectonic activity driven by the collision of the Indian and Eurasian plates. The regional tectonic framework is primarily controlled by major fault systems, notably the Main Central Thrust (MCT) and the Southern Tibet Detachment System (STDS) [66].

Tectonic uplift of the Himalayas has shaped the steep terrain and intensified the Asian monsoon circulation, thereby creating critical topographical and climatic prerequisites for the widespread formation of glaciers and glacial lakes [67,68]. The Himalayas currently contain 20,431 glaciers, with a combined area of approximately 19,679 km^2 [59]. In the Nyainqentanglha Mountains, approximately 6860 glaciers cover an area of 9600 km^2, representing a glacial lake volume of 835.3 $\pm$ 31.3 km^3 [69]. In recent decades, proglacial lakes in this region have exhibited rapid expansion. Between 1990 and 2020, the number of proglacial lakes in the Himalayas increased by an average of 155 per decade, with the total surface area expanding by 20.9 $\pm$ 1.02 km^2 decadally. This trend accelerated between 2000 and 2020, marked by a decadal increase of 179 lakes and an area expansion of 23.83 $\pm$ 1.55 km^2 [31]. The study area encompasses multiple countries, including China, Nepal, Bhutan, India, and Pakistan, and supports a population of tens of millions. Critical infrastructure, exemplified by the Qinghai–Tibet, Sichuan–Tibet, and China–Nepal railways, traverses this region. GLOFs pose substantial threats to infrastructure and socioeconomic stability [21]. Although the recent frequency of GLOFs in the Himalayas remains debated, multiple studies project an increase in their occurrence in the coming decades [12,70,71]. Accelerated glacier retreat, intense erosion, weathering, and active tectonics collectively foster conditions conducive to GLOFs. Consequently, precise quantification of glacial lake volume and maximum depth, alongside a rigorous assessment of outburst hazards and potential downstream impacts, is imperative for regional disaster risk reduction and sustainable development.

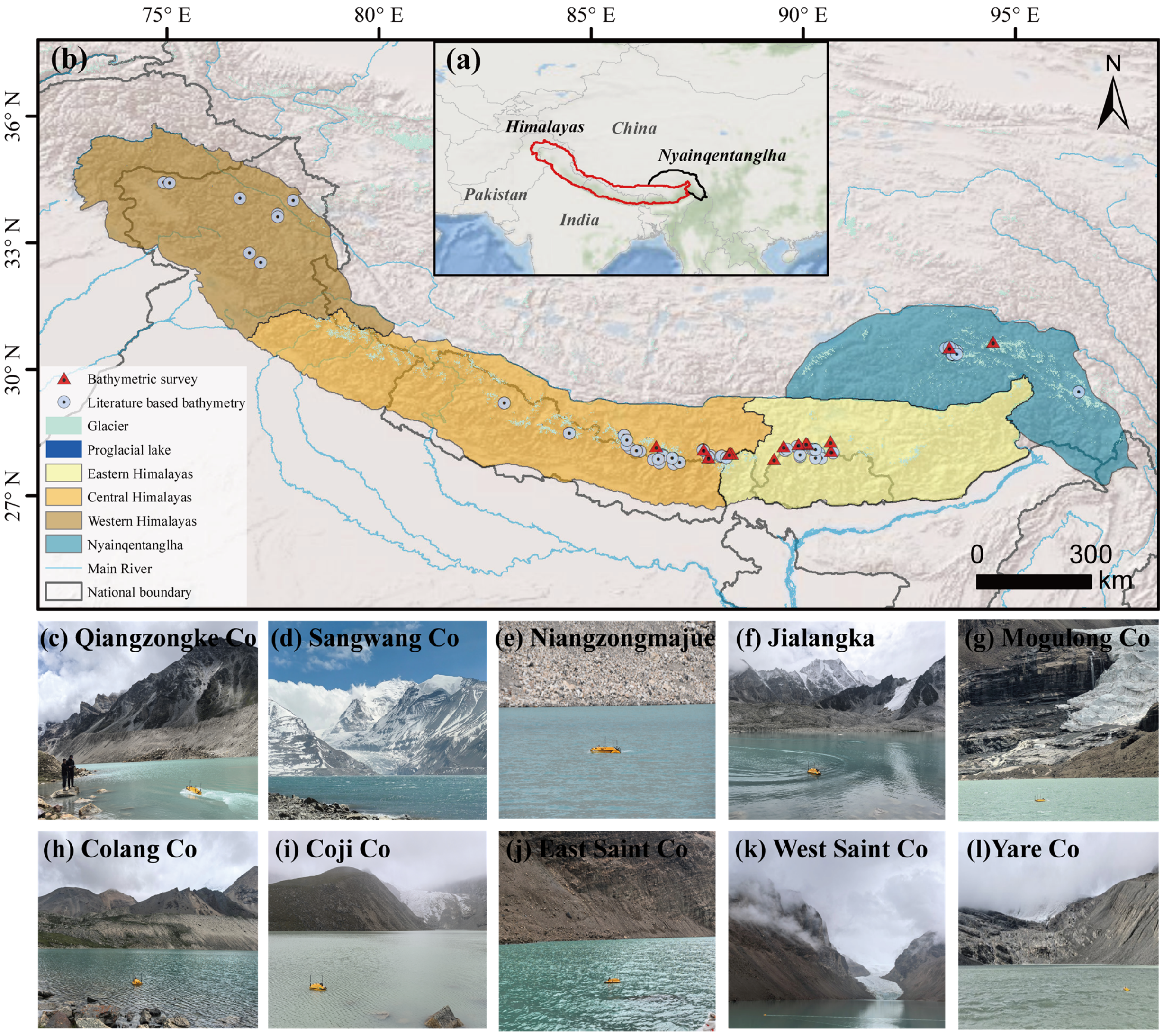

Figure 1. Geographical setting of the study area, (**a**) location of the Himalaya and Nyainqentanglha Ranges within High Mountain Asia, (**b**) spatial distribution of glaciers, proglacial lakes, and lake depth measurement sites, (**c**–**l**) photographs of in situ bathymetric surveys conducted in this study.

3. Data and Methods

This study was conducted following the technical workflow (Figure 2). First, high-quality in situ bathymetric records of proglacial lakes across the Himalaya and Nyainqentanglha ranges were systematically collected from published literature and integrated with field survey data obtained in this study. All lake samples included in the analysis were measured using consistent types of bathymetric equipment, thereby guaranteeing the accuracy and uniformity of the original data. The integrated samples were compiled into a comprehensive dataset, which was randomly divided into a modeling subset and an independent validation subset at a ratio of 8:2. Based on the power–law function, regional empirical relationships between lake area and water storage were established for proglacial lakes in the study area. Second, relying on the existing historical vector dataset of proglacial lakes, the OTSU threshold segmentation method combined with visual interpretation was adopted to extract and reconstruct the long-term lake area time series from 1990 to 2020. Subsequently, the validated area–storage empirical formula was applied to estimate the water storage of individual proglacial lakes using interpreted lake area data. Finally, the spatiotemporal variation characteristics of proglacial lake water storage over the past 30 years were systematically analyzed.

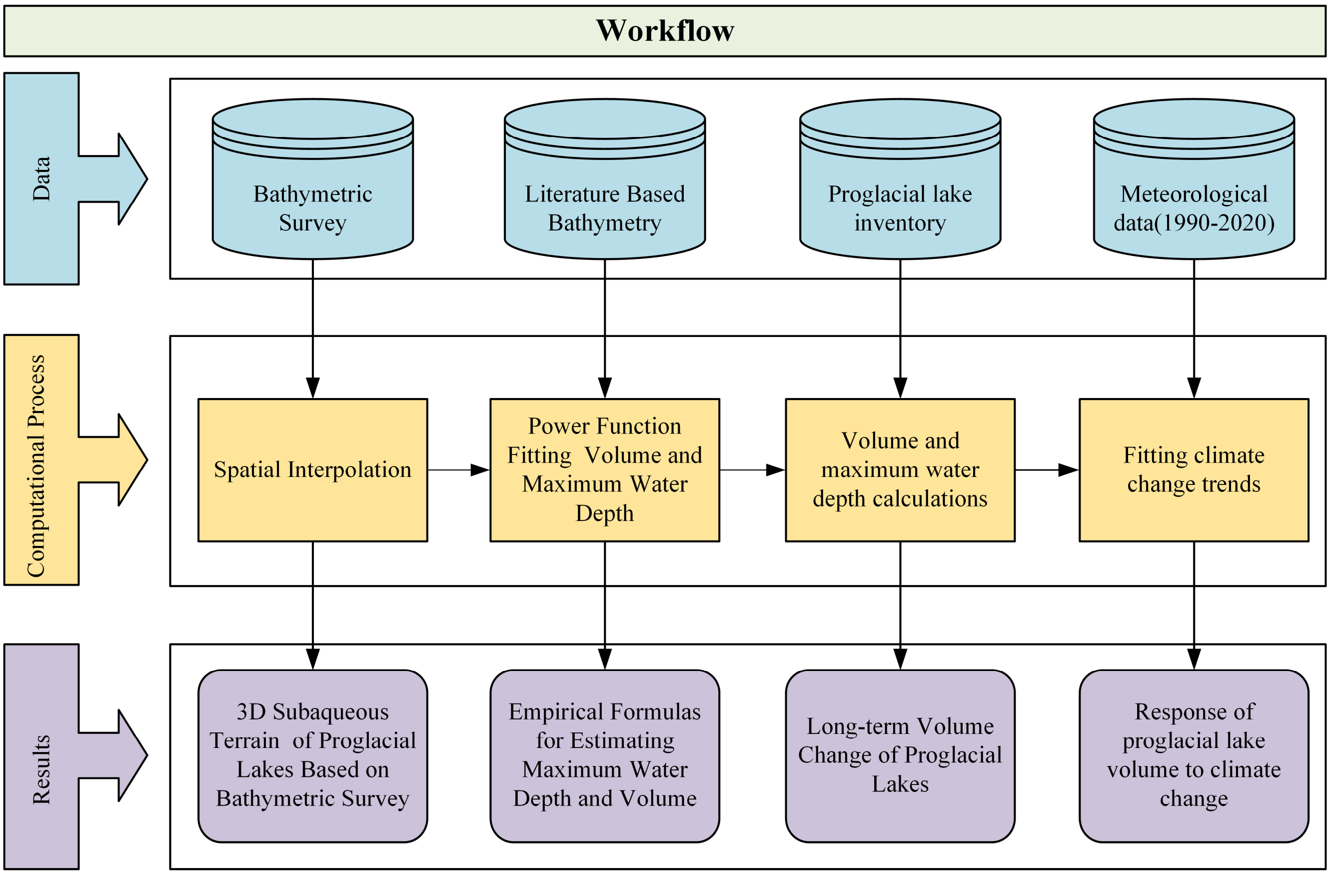

Figure 2. Workflow of the research methodology.

3.1. Bathymetric Data Acquisition and Model Development

High summer temperatures result in ice-free conditions on glacial lakes, rendering this period optimal for hydrographic surveys. Accordingly, in situ bathymetric surveys were conducted on ten representative glacial lakes in the Himalaya and Nyainqentanglha ranges between July and September 2024 (Figure 1b). The study sites include Qiangzongke Co, Sangwang Co, Niangzongmajue, Jialangka, Mogulong Co, Cuolang Co, Cuoji Co, East Saint Co, West Saint Co, and Yare Co (Figure 1c–l). Bathymetric surveys were conducted using the Apache 3 Pro USV (Huace Navigation Technology Co., Ltd., Shanghai, China) equipped with a 200 kHz single-beam echo sounder. The instrument provides a depth measurement range of 0.1–300 m, with a vertical accuracy of ±1 cm, a vertical resolution of 1 cm, and a sampling frequency up to 30 Hz. The USV is also fitted with dual global navigation satellite system antennas for high-precision positioning and an autonomous obstacle avoidance system. Bathymetric data were collected automatically along pre-designed survey transects (Figure 3).

After data quality control and outlier elimination, this study established an integrated dataset comprising 79 valid samples for proglacial lake volume estimation and 45 valid samples for maximum water depth estimation (Supplementary Materials). Both datasets were randomly partitioned at an 8:2 ratio for model calibration and independent validation (Figure 2). Existing studies have confirmed stable power–law relationships between glacial lake area, volume and maximum depth [30,39]. Accordingly, this study established regionally adapted empirical models to estimate the volume and maximum depth of proglacial lakes across the Himalaya and Nyainqentanglha ranges (Figure 2). Monthly meteorological data covering 1990–2020 were retrieved from the Climate Research Unit (CRU) with a spatial resolution of 0.5° × 0.5°.

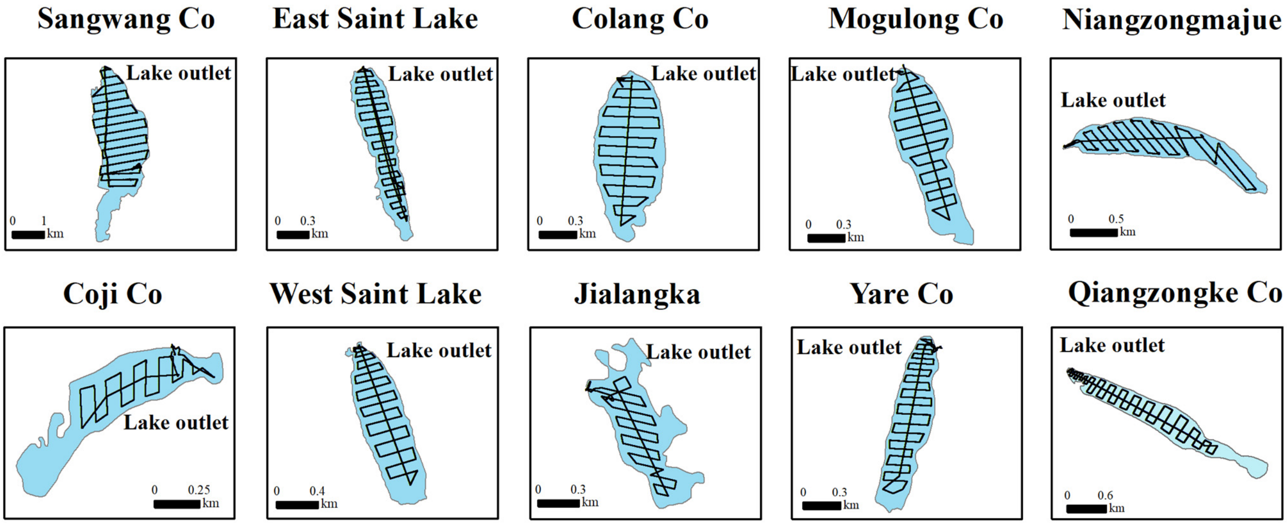

Figure 3. Spatial distribution of USV survey tracks across the studied proglacial lakes.

3.2. Bathymetric Data Processing and Volume Estimation

The in situ bathymetric data acquired from the proglacial lake were processed and analyzed using Hydrosurvey and ArcGIS Pro 3.6 software. First, raw sonar returns recorded by the USV were initially imported into Hydrosurvey for pre-processing, which entailed filtering and smoothing protocols to remove spurious data points and minimize signal noise. Next, the processed depth points were subsequently imported into ArcGIS Pro 3.6. Continuous bathymetric surfaces were generated by IDW interpolation at a fixed 5 m grid resolution. Suitable for the gentle lake-bottom terrain, IDW is widely used in glacial lake studies [31]. The 5 m resolution balances topographic accuracy and computational efficiency based on USV survey conditions. Finally, lake storage volume was computed using the Surface Volume tool within ArcGIS Pro 3.6.

3.3. Error Estimation

The accuracy of the empirical formula for predicting glacial lake volume and maximum water depth was evaluated using four standard statistical metrics: bias, mean absolute percentage error (MAPE), coefficient of determination (R^2), and root mean squared error (RMSE). The specific calculation formulas are presented in expressions (1)–(4). In these equations, n represents the number of samples, $\hat{y}_i$ refers to the predicted result for the i-th sample, y_i represents the corresponding observed value, and $\overline{y}$ indicates the mean of the measured samples.

$$Bias = \frac{1}{n}\sum_{i=1}^{n}(\hat{y}_i - y_i) \tag{1}$$

$$MAPE = \frac{1}{n}\sum_{i=1}^{n}\left|\frac{\hat{y}_i - y_i}{y_i}\right| \times 100\% \tag{2}$$

$$R^2 = 1 - \left[\sum_{i=1}^{n}(y_i - \hat{y}_i)^2 / \sum_{i=1}^{n}(y_i - \overline{y})^2\right] \tag{3}$$

$$RMSE = \sqrt{\frac{1}{n}\sum_{i=1}^{n}(y_i - \hat{y}_i)^2} \tag{4}$$

The accuracy of proglacial lake volume estimation critically depends on the precision of input parameters, especially the delineation of lake surface extent. However, the finite spatial resolution of remote sensing imagery inevitably limits the precision of boundary extraction, introducing propagation errors. Consequently, rigorous quantification of boundary delineation errors is imperative to constrain the reliability of volumetric uncertainty assessments.

$$\delta = \frac{P}{G} \times \frac{G^2}{2} \times 0.6872 \quad (5)$$

In the expression (5), δ represents the error range of the proglacial lake area (m^2), P denotes the perimeter of the proglacial lake (m), and G indicates the spatial resolution of the remote sensing imagery used (m).

4. Results

4.1. Morphometric Characteristics of Surveyed Proglacial Lakes

High-resolution in situ bathymetric surveys were conducted using an USV to map the underwater topography of proglacial lakes across the Himalaya and Nyainqentanglha ranges (Figure 3). This effort yielded accurate measurements of water volume and maximum depth for 10 representative lakes (Table 1). The surveyed lakes displayed significant morphometric diversity, with surface areas ranging from 0.30 to 6.02 km^2, volumes from 5.40×10^6 to 435.44×10^6 m^3, and maximum depths between 34.18 and 137.64 m. Strong positive correlations were observed between lake area, volume, and depth, suggesting that larger proglacial lakes consistently harbor greater volumetric capacities and deeper basins.

Table 1. Measured Water Depths of 10 Glacial Lakes in the Himalaya and Nyainqentanglha.

Name	Longitude	Latitude	Area (km^2)	Volume (10^6 m^3)	Maximum Depth (m)
Sangwang Co	90.11	28.24	6.02 ± 0.005	435.44	137.64
Qiangzongke Co	87.77	27.93	1.07 ± 0.003	43.05	80.02
Niangzongmajue	86.53	28.19	0.67 ± 0.002	22.02	63.77
East Saint Lake	88.26	28.01	0.64 ± 0.001	29.02	70.73
Cuolang Co	89.31	27.88	0.62 ± 0.001	27.05	81.21
Mogulong Co	88.29	28.02	0.50 ± 0.001	11.82	45.27
West Saint Lake	88.24	28.01	0.44 ± 0.001	11.46	42.69
Jialangka	90.65	28.07	0.40 ± 0.002	5.40	37.86
Yare Co	88.32	28.01	0.37 ± 0.001	7.42	34.18
Cuoji Co	90.65	28.30	0.30 ± 0.001	7.01	44.60

4.2. Empirical Area–Volume and Area–Maximum Depth Scaling Relationships

In situ bathymetric surveys were executed at 10 representative glacial lakes to quantitatively delineate the basin morphometry of each lake (Figure 4). All valid samples were randomly partitioned into an 80% calibration subset for model fitting and a 20% independent validation subset for accuracy assessment, with a strict 8:2 splitting ratio adopted for both lake volume and maximum depth datasets. Nonlinear regression analysis of these data points established power–law scaling relationships between lake volume (V) and area (A) (Figure 5a), as well as between maximum water depth (D) and area (A) for proglacial lakes across the Himalaya and Nyainqentanglha ranges (Figure 5b). The derived empirical equations are presented as Equations (6) and (7).

$$V = 43.37\ A^{1.2838} \quad (6)$$

$$D = 95.65\ A^{0.7851} \quad (7)$$

In the equation above, V represents proglacial lake volume (10^6 m^3); A denotes surface area (km^2); and D corresponds to the maximum water depth (m). These scaling relationships quantitatively characterize the dependencies among the morphometric parameters of proglacial lakes. A non-linear, positive correlation is observed between lake volume and surface area (Figure 5a), indicating that volume scales disproportionately with areal expansion. The majority of data points from both the current study and previous investigations fall within the 95% confidence interval, signifying a robust fit of the proposed model. Furthermore, a concomitant increase in maximum depth relative to lake surface area is evident in the scaling relationship (Figure 5b). Overall, the model exhibits superior fitting accuracy and reliable predictive capability within the calibrated range.

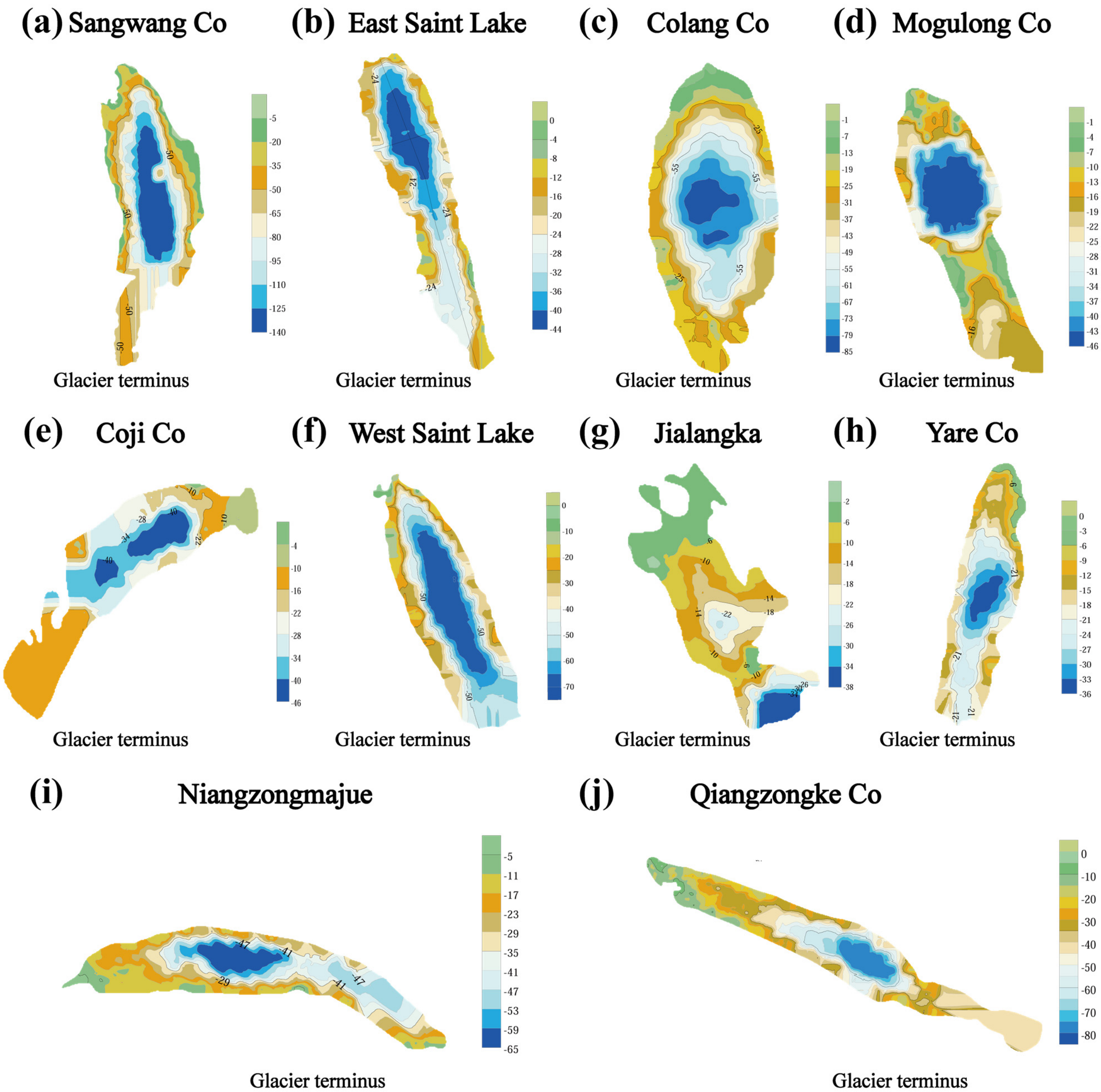

Figure 4. Bathymetry of proglacial lakes surveyed in the Himalaya and Nyainqentanglha ranges: (**a**) Sangwang Co, (**b**) East Saint Co, (**c**) Cuolang Co, (**d**) Mogulong Co, (**e**) Cuoji Co, (**f**) West Saint Co, (**g**) Jialangka, (**h**) Yare Co, (**i**) Niangzongmajue, and (**j**) Qiangzongke Co.

4.3. Performance Evaluation Against Existing Empirical Models

Worldwide, numerous empirical equations have been established to quantify the maximum water depth and volume of glacial lakes [30,39,40,50,58,72–74]. These formulations rely on the positive correlation among surface area, volume, and maximum depth, leading to nonlinear empirical relationships with robust fitting performance. However, due to divergent regional topography, basin morphometry, and lake type [45], these scaling relationships exhibit pronounced spatial heterogeneity. Consequently, this complexity necessitates the calibration of empirical models when assessing proglacial lake volumes across distinct geographic regions [39]. Prevalent global volume estimates are predominantly derived from empirical equations originally calibrated for the European Alps and the Andes. Nevertheless, the direct application of these extrinsic models to proglacial lakes in the Himalaya and Nyainqentanglha results in significant prediction errors. Although previous studies have incorporated multiple morphometric variables, including lake area, length, and width, to estimate glacial lake volume and maximum water depth [31,32], surface area remains the primary and most practical predictor for volumetric assessment [30,39]. Consequently, the present study systematically evaluates the proposed empirical formula through a comprehensive comparison with 14 volume estimation formulas and 6 maximum water depth equations established in existing literature. The results quantify the performance differences among various empirical formulas for estimating proglacial lake volume and maximum water depth (Table 2).

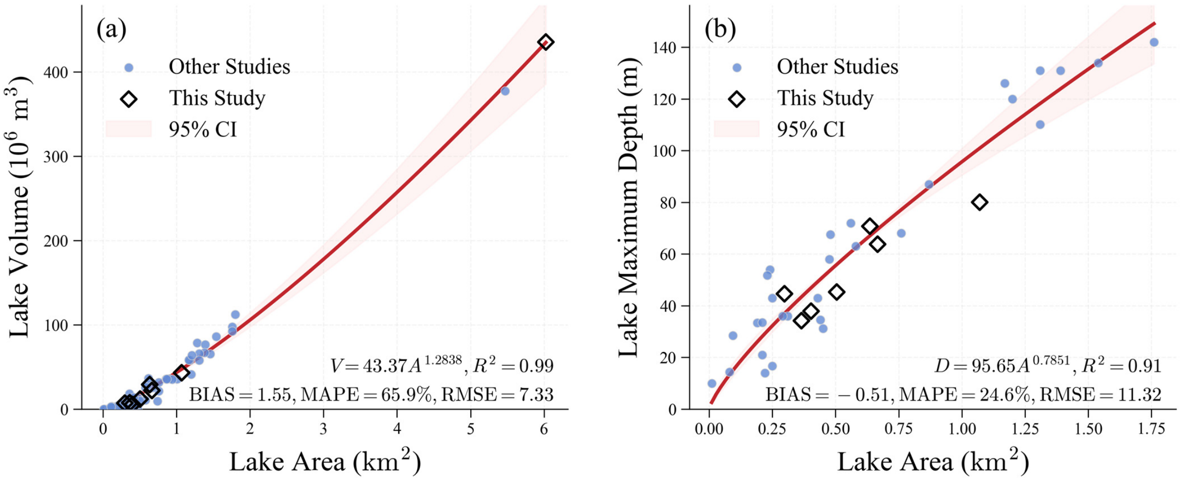

Figure 5. Empirical equations for estimating lake volume and maximum depth from the area in the Himalaya and Nyainqentanglha ranges, (**a**) Volume estimation, (**b**) Maximum depth estimation.

Table 2. Empirical equations for estimating volume and maximum water depth.

	Formulas	**Code**	**N**	**Empirical Formula**	R^2
Estimating Volume	This study	Equation (1)	64		0.99
	Evans [52]	Equation (2)	/	V = 0.035 $A^{1.5}$	/
	Popov [73]	Equation (3)	/	V = 0.059 $A^{1.44}$	/
	Huggel et al. [51]	Equation (4)	15	V = 0.104 $A^{1.42}$	0.92
	Sakai [50]	Equation (5)	15	V ($\times 10^6$ m^3) = 43.24 $A^{1.5307}$	/
	Wang et al. [49]	Equation (6)	20	V = 0.087 $A^{1.434}$	0.50
	Loriaux and Casassa [48]	Equation (7)	31	V = 0.2933 $A^{1.3324}$	0.96
	Emmer and Vilímek [74]	Equation (8)	35	V = 0.054393 $A^{1.483009}$	0.92
	Cook and Quincey [45]	Equation (9)	30	V = 0.1746 $A^{1.3725}$	0.60
	Khanal et al. [46]	Equation (10)	33	V = 0.0578 $A^{1.5}$	0.93
	Zhang et al. [31]	Equation (11)	59	V ($\times 10^6$ m^3) = 42.95 $A^{1.408}$	0.99
	Patel et al. [44]	Equation (12)	17	V ($\times 10^6$ m^3) = 40 A^2 + 5.06 A	0.96
	Kapitsa et al. [43]	Equation (13)	32	V = 0.036 $A^{1.49}$	/
	Watson et al. [42]	Equation (14)	24	V = 0.1389 $A^{1.4016}$	0.98
	Wood et al. [41]	Equation (15)	170	V = 0.126 $A^{1.412}$	0.83
Estimating Maximum Depth	This Study	Equation (1)	36		0.91
	Sakai [50]	Equation (2)	15	D = 95.665 $A^{0.489}$	/
	Fujita et al. [72]	Equation (3)	/	D = 55 $A^{0.25}$	/
	Zhang et al. [57]	Equation (4)	40	D = 99.99 $A^{0.51}$	0.86
		Equation (5)	64	D = 97.16 $A^{0.55}$	0.53
		Equation (6)	26	D = 52.14 $A^{0.33}$	0.85
		Equation (7)	8	D = 100.02 $A^{0.47}$	0.82

The empirical formula proposed in this study outperforms existing models for proglacial lake volume estimation, with superior bias, R^2 and RMSE values and a competitive MAPE (Figure 6). Bias values from previous equations range from -14.68×10^6 to -1.36×10^6 m^3. Our formula yields the smallest absolute bias with a value of -1.17×10^6 m^3, which greatly mitigates the systematic underestimation commonly reported in prior studies (Figure 6a). MAPE values for Equations 3–16 range from 12.9% to 44.1%, while our model achieves a MAPE of 13.2% (Figure 6b). Although a marginally lower MAPE of 12.9% was reported in the study by Zhang et al. [31], our model reaches a coefficient of determination of 0.936, which is higher than the coefficient of determination values of all other available models that lie between 0.896 and 0.934 (Figure 6c). In addition, our formula produces the lowest RMSE at 4.58×10^6 m^3. This value is around 12.7% lower than the best-performing existing model and approximately 3.6 times smaller than the least accurate model proposed by Popov [73], whose root mean square error is 16.39×10^6 m^3 (Figure 6d).

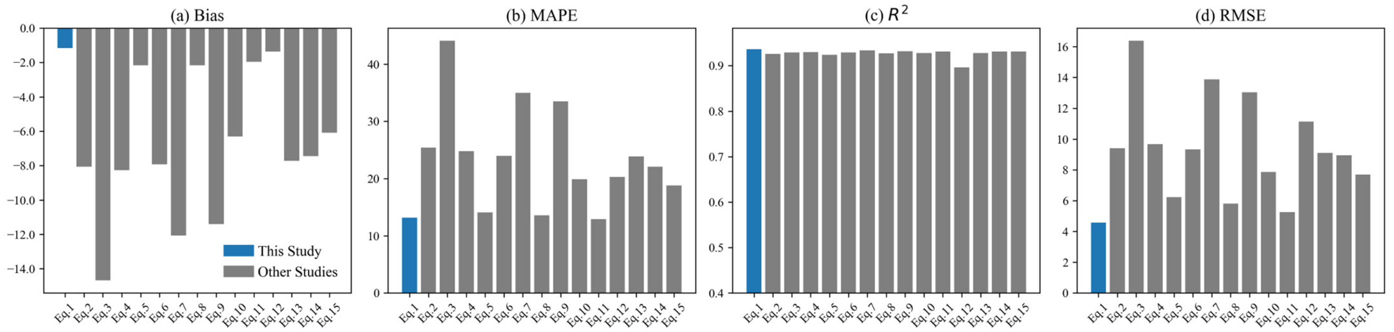

Figure 6. Statistical evaluation of volume estimation formulas, (**a**) Bias, (**b**) Mean Absolute Percentage Error (MAPE), (**c**) Coefficient of Determination (R^2), (**d**) Root Mean Square Error (RMSE).

Furthermore, the newly constructed formula also outperforms existing methods for estimating the maximum water depth of proglacial lakes, with lower values in absolute bias, MAPE and RMSE (Figure 7). Our model obtains an absolute bias of 1.05 m. This value is much lower than the bias values of Equations 2–7, which range from 6.72 m to −29.88 m (Figure 7a). The MAPE of existing formulas ranges from 13.6% to 36.2%, while the proposed method reaches 10%, an improvement of at least 26.5% relative to the optimal existing model reported by Sakai [50] (Figure 7b). The R^2 of previous models varies between 0.703 and 0.716, and our value of 0.692 remains at a comparable explanatory capacity (Figure 7c). In terms of prediction error, our formula yields an RMSE of 8.58 m. This figure is 21.6% lower than the smallest RMSE of 10.94 m from other empirical equations, and over three times lower than that of the least reliable models (Figure 7d).

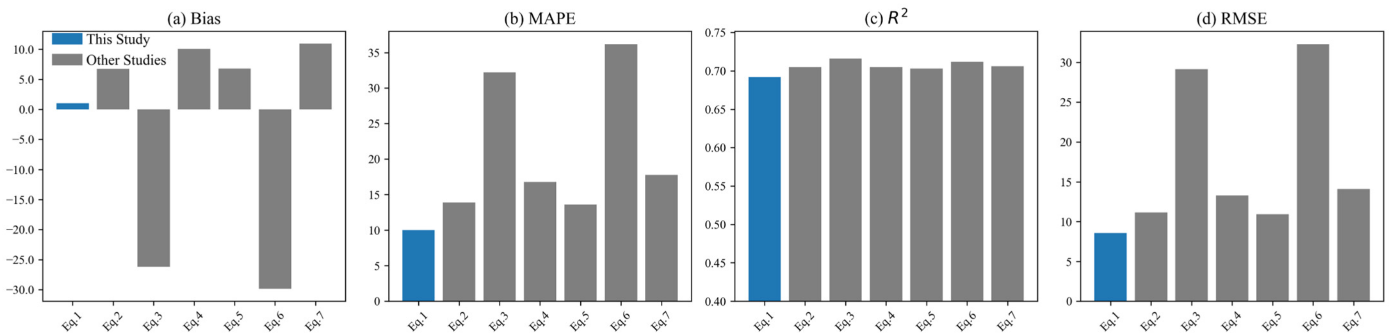

Figure 7. Statistical evaluation of maximum water depth estimation formulas, (**a**) Bias, (**b**) Mean Absolute Percentage Error (MAPE), (**c**) Coefficient of Determination (R^2), (**d**) Root Mean Square Error (RMSE).

4.4. Response of Proglacial Lake Volume to Climate Change

Spatiotemporal trends in meteorological variables across the Himalaya and Nyainqentanglha regions were evaluated using time series data from 1990 to 2020. Mean annual air temperature exhibits a general upward trend, with an average annual warming rate of 0.0286 °C (Figure 8a), and the spatial variation in air temperature is statistically significant ($p < 0.05$). Notably, significant warming was evident in the Western Himalayas and Nyainqentanglha Mountains, whereas the Eastern Himalayas and western Central Himalayas demonstrated more attenuated increases. Conversely, a localized cooling trend was detected in the eastern Central Himalayas (Figure 8b).

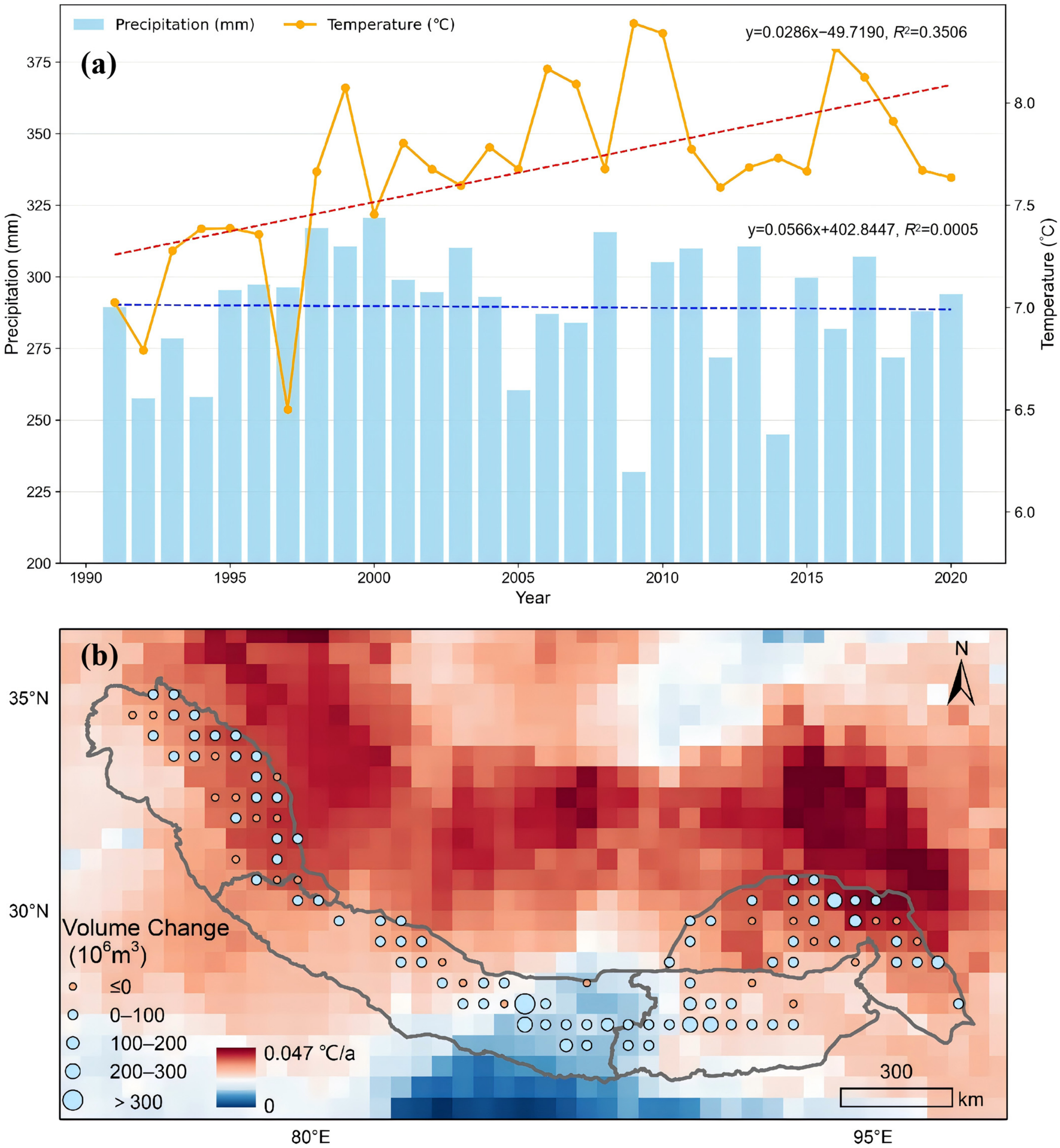

Figure 8. Climate change and proglacial lake volume evolution in the Himalaya and Nyainqentanglha Ranges from 1990 to 2020, (**a**) Interannual trends in mean annual temperature and annual precipitation, (**b**) response of proglacial lake volume to mean annual temperature variations. The circle size represents the annual rate of change in proglacial lake volume within 0.5° × 0.5° grid cells.

Proglacial lakes in the region have exhibited a sustained volumetric expansion from 1990 to 2020 (Figure 8b). In the Western Himalayas, aggregate volume increased by 46.7%, expanding from $199.80 \pm 28.76 \times 10^6$ m^3 in 1990 to $293.03 \pm 47.47 \times 10^6$ m^3 in 2020. The Central Himalayas demonstrated a comparable relative expansion of 46.4%, increasing from $2862.30 \pm 194.59 \times 10^6$ m^3 to $4190.59 \pm 283.42 \times 10^6$ m^3 over the same period. Meanwhile, the Eastern Himalayas recorded a 51.5% volume increase for proglacial lakes, with total storage rising from $1285.01 \pm 92.89 \times 10^6$ m^3 to $1946.11 \pm 166.74 \times 10^6$ m^3. The Nyainqentanglha Mountains exhibited the most pronounced change, with a 92.9% increase in volume, growing from $813.14 \pm 73.75 \times 10^6$ m^3 in 1990 to $1568.39 \pm 121.95 \times 10^6$ m^3 in 2020. This regional heterogeneity highlights that while the Central Himalayas contain the largest concentration of lakes, they exhibited the lowest relative rate of expansion; conversely, the Nyainqentanglha Mountains demonstrated the most rapid growth. The expansion is primarily attributed to rising temperatures that accelerate glacier ablation, generating sustained meltwater runoff and consequent lake enlargement. Furthermore, basin bathymetry and glacier geometry, alongside evaporation rates, modulate the spatiotemporal variability of these volumetric fluctuations.

5. Discussion

The empirical models developed in this study are specifically applicable to the Himalaya and Nyainqentanglha regions. While these equations exhibit strong robustness within this spatial scope, their direct application to regions with distinct geomorphological characteristics may introduce considerable uncertainty. Therefore, extending the application of these models to other regions requires recalibration with region-specific topographical and hydrological parameters. Key covariates critical to this recalibration process include lake morphology, turbidity, parent glacier type, and dam type, whose integration can significantly improve the accuracy of glacial lake volume estimation.

Quantifying the uncertainty associated with glacial lake volume and maximum depth is essential for ensuring the reliability of these parameters. Such assessments directly affect the susceptibility analysis of GLOFs and the robustness of numerical simulation scenarios [8,12,27]. Estimation uncertainty originates from multiple sources, including the quality of input data and environmental variability induced by climate change. Notably, the glacial lake area, as a core input parameter for estimating lake volume and maximum depth, is subject to non-negligible uncertainties, which primarily stem from the spatial resolution limitations of remote sensing imagery, subjective biases in manual visual interpretation, and the inherent ambiguity of the Otsu threshold segmentation algorithm. Using Equation 5 proposed in this study, such area extraction uncertainties can be quantitatively calculated and further propagated to the estimations of lake volume and maximum depth through the established area–volume and area–maximum depth empirical relationships, thereby leading to discrepancies between modelled results and actual in situ measurements. Furthermore, the complexity of regional topography, along with the physical and dynamic characteristics of the parent glacier, introduces substantial uncertainty. Additionally, the estimation results depend on the morphometric and hydrological properties of the glacial lake, as well as the sediment transport and deposition processes within the lake [39,75–77].

6. Conclusions

This study integrated historical documentation with field measurements of proglacial lakes to establish empirical formulas for predicting proglacial lake volume and maximum depth in the Himalaya and Nyainqentanglha regions. A comprehensive statistical evaluation demonstrated that the derived empirical formula achieved the highest R^2 value and the lowest bias, MAPE, and RMSE, thereby providing a robust tool for estimating these parameters regionally. Substantial increases in proglacial lake volume were observed between 1990 and 2020, primarily attributed to climatic warming, with regional expansion rates of approximately 92.9% in the Nyainqentanglha Mountains, 51.5% in the Eastern Himalayas, 46.4% in the Central Himalayas, and 46.7% in the Western Himalayas. These findings collectively quantify the considerable sensitivity of proglacial lakes to climate change in this region. In addition, the precise volume and maximum water depth data obtained using the methodology presented in this study are critical for significantly enhancing the accuracy of GLOF numerical simulations in the Himalaya and Nyainqentanglha regions, which also provides the scientific basis for effective GLOF risk mitigation and the development of climate change adaptation strategies.

Supplementary Materials: The following supporting information can be downloaded at: https://www.mdpi.com/article/10.3390/rs18132249/s1, Table S1: Summary of the 79 bathymetric datasets used to develop the new volume estimation equation; Table S2: Summary of the 45 bathymetric datasets used to develop the new maximum depth estimation equation.

Author Contributions: Conceptualization, M.Z.; Methodology, M.Z., H.W., Y.Y. and J.C.; Software, M.Z., J.T., J.Y. and Q.L.; Formal analysis, M.Z., J.T. and Y.Y.; Investigation, M.Z., H.W., J.C. and X.L.; Resources, P.C., J.Y. and Y.L.; Data curation, M.Z., Y.Y., Y.L. and Q.L.; Writing—original draft, M.Z.; Writing—review & editing, H.W., P.C. and J.T.; Visualization, J.C. and X.L.; Supervision, P.C.; Funding acquisition, H.W. All authors have read and agreed to the published version of the manuscript.

Funding: This research was supported by the Science and Technology Project of Power China (DJ-HXGG-2022-02), the Key Laboratory of Mountain Hazards and Engineering Resilience, Institute of Geographic Sciences and Natural Resources Research, Chinese Academy of Sciences (KLMHER-T01).

Data Availability Statement: The original contributions presented in the study are included in the article, further inquiries can be directed to the corresponding author.

Conflicts of Interest: Authors Jingxi Yang, Yunpeng Liu and Qingchun Li were employed by the company POWERCHINA Chengdu Engineering Corporation Limited. The remaining authors declare that the research was conducted in the absence of any commercial or financial relationships that could be construed as a potential conflict of interest.

References

1. Zemp, M.; Jakob, L.; Dussaillant, I.; Nussbaumer, S.U.; Gourmelen, N.; Dubber, S.; Geruo, A.; Abdullahi, S.; Andreassen, L.M.; Berthier, E.; et al. Community Estimate of Global Glacier Mass Changes from 2000 to 2023. *Nature* **2025**, *639*, 382–388. [CrossRef]
2. Chen, D.; Xu, B.; Yao, T. Assessment of Past, Present and Future Environmental Changes on the Tibetan Plateau. *Chin. Sci. Bull.* **2015**, *60*, 3025–3035. [CrossRef]
3. Yao, T.; Xue, Y.; Chen, D.; Chen, F.; Thompson, L.; Cui, P.; Koike, T.; Lau, W.K.-M.; Lettenmaier, D.; Mosbrugger, V.; et al. Recent Third Pole's Rapid Warming Accompanies Cryospheric Melt and Water Cycle Intensification and Interactions between Monsoon and Environment: Multidisciplinary Approach with Observations, Modeling, and Analysis. *Bull. Am. Meteorol. Soc.* **2019**, *100*, 423–444. [CrossRef]
4. Yao, T.; Bolch, T.; Chen, D.; Gao, J.; Immerzeel, W.; Piao, S.; Su, F.; Thompson, L.; Wada, Y.; Wang, L.; et al. The Imbalance of the Asian Water Tower. *Nat. Rev. Earth Environ.* **2022**, *3*, 618–632. [CrossRef]
5. Yao, X.; Liu, S.; Han, L.; Sun, M.; Zhao, L. Definition and Classification System of Glacial Lake for Inventory and Hazards Study. *J. Geogr. Sci.* **2018**, *28*, 193–205. [CrossRef]
6. Du, C.; Zhang, K.; Lin, Q.; Huang, S.; Han, Y.; Ren, J.; Xing, P.; Liu, J.; Taylor, D.; Shen, J. Rapid Ecological Change Outpaces Climate Warming in Tibetan Glacier Lakes. *Commun. Earth Environ.* **2025**, *6*, 523. [CrossRef]
7. Shugar, D.H.; Burr, A.; Haritashya, U.K.; Kargel, J.S.; Watson, C.S.; Kennedy, M.C.; Bevington, A.R.; Betts, R.A.; Harrison, S.; Strattman, K. Rapid Worldwide Growth of Glacial Lakes since 1990. *Nat. Clim. Change* **2020**, *10*, 939–945. [CrossRef]
8. Zhang, T.; Wang, W.; An, B.; Wei, L. Enhanced Glacial Lake Activity Threatens Numerous Communities and Infrastructure in the Third Pole. *Nat. Commun.* **2023**, *14*, 8250. [CrossRef]
9. Brun, F.; Wagnon, P.; Berthier, E.; Jomelli, V.; Maharjan, S.B.; Shrestha, F.; Kraaijenbrink, P.D.A. Heterogeneous Influence of Glacier Morphology on the Mass Balance Variability in High Mountain Asia. *J. Geophys. Res. Earth Surf.* **2019**, *124*, 1331–1345. [CrossRef]

10. King, O.; Bhattacharya, A.; Bhambri, R.; Bolch, T. Glacial Lakes Exacerbate Himalayan Glacier Mass Loss. *Sci. Rep.* **2019**, *9*, 18145. [CrossRef]
11. Watson, C.S.; Kargel, J.S.; Shugar, D.H.; Haritashya, U.K.; Schiassi, E.; Furfaro, R. Mass Loss from Calving in Himalayan Proglacial Lakes. *Front. Earth Sci.* **2020**, *7*, 342. [CrossRef]
12. Zheng, G.; Allen, S.K.; Bao, A.; Ballesteros-Cánovas, J.A.; Huss, M.; Zhang, G.; Li, J.; Yuan, Y.; Jiang, L.; Yu, T.; et al. Increasing Risk of Glacial Lake Outburst Floods from Future Third Pole Deglaciation. *Nat. Clim. Change* **2021**, *11*, 411–417. [CrossRef]
13. Luo, Y.; Yin, Y.; Zhong, Y.; Lu, X.; Yang, J.; Sapkota, L.; Lu, X.; Liu, Q. Dynamics of Lake-Terminating Glaciers in the Himalaya and Southeastern Tibet between 1990 and 2020. *J. Glaciol.* **2025**, *71*, e113. [CrossRef]
14. Neupane, R.; Chen, H.; Cao, C. Review of Moraine Dam Failure Mechanism. *Geomat. Nat. Hazards Risk* **2019**, *10*, 1948–1966. [CrossRef]
15. Sattar, A.; Cook, K.L.; Rai, S.K.; Berthier, E.; Allen, S.; Rinzin, S.; de Vries, M.V.W.; Haeberli, W.; Kushwaha, P.; Shugar, D.H.; et al. The Sikkim Flood of October 2023: Drivers, Causes, and Impacts of a Multihazard Cascade. *Science* **2025**, *387*, eads2659. [CrossRef]
16. Yang, L.; Lu, Z.; Zhao, C.; Zhang, Q.; Hu, X.; Wang, B. Triggering Factors and Flooding Processes of Glacial Lake Outburst Flood at Ranzerio Lake. *npj Nat. Hazards* **2025**, *2*, 90. [CrossRef]
17. Zhang, G.; Carrivick, J.L.; Emmer, A.; Shugar, D.H.; Veh, G.; Wang, X.; Labedz, C.; Mergili, M.; Mölg, N.; Huss, M.; et al. Characteristics and Changes of Glacial Lakes and Outburst Floods. *Nat. Rev. Earth Environ.* **2024**, *5*, 447–462. [CrossRef]
18. Peng, M.; Wang, X.; Zhang, G.; Veh, G.; Sattar, A.; Chen, W.; Allen, S. Cascading Hazards from Two Recent Glacial Lake Outburst Floods in the Nyainqêntanglha Range, Tibetan Plateau. *J. Hydrol.* **2023**, *626*, 130155. [CrossRef]
19. Veh, G.; Korup, O.; Walz, A. Hazard from Himalayan Glacier Lake Outburst Floods. *Proc. Natl. Acad. Sci. USA* **2020**, *117*, 907–912. [CrossRef] [PubMed]
20. Cook, K.L.; Andermann, C.; Gimbert, F.; Adhikari, B.R.; Hovius, N. Glacial Lake Outburst Floods as Drivers of Fluvial Erosion in the Himalaya. *Science* **2018**, *362*, 53–57. [CrossRef] [PubMed]
21. Taylor, C.; Robinson, T.R.; Dunning, S.; Rachel Carr, J.; Westoby, M. Glacial Lake Outburst Floods Threaten Millions Globally. *Nat. Commun.* **2023**, *14*, 487. [CrossRef]
22. Sattar, A.; Haritashya, U.K.; Kargel, J.S.; Karki, A. Transition of a Small Himalayan Glacier Lake Outburst Flood to a Giant Transborder Flood and Debris Flow. *Sci. Rep.* **2022**, *12*, 12421. [CrossRef]
23. Meyrat, G.; Munch, J.; Cicoira, A.; McArdell, B.; Müller, C.R.; Frey, H.; Bartelt, P. Simulating Glacier Lake Outburst Floods (GLOFs) with a Two-Phase/Layer Debris Flow Model Considering Fluid-Solid Flow Transitions. *Landslides* **2024**, *21*, 479–497. [CrossRef]
24. Wang, X.; Zhang, G.; Veh, G.; Sattar, A.; Wang, W.; Allen, S.K.; Bolch, T.; Peng, M.; Xu, F. Reconstructing Glacial Lake Outburst Floods in the Poiqu River Basin, Central Himalaya. *Geomorphology* **2024**, *449*, 109063. [CrossRef]
25. Allen, S.K.; Sattar, A.; King, O.; Zhang, G.; Bhattacharya, A.; Yao, T.; Bolch, T. Glacial Lake Outburst Flood Hazard under Current and Future Conditions: Worst-Case Scenarios in a Transboundary Himalayan Basin. *Nat. Hazards Earth Syst. Sci.* **2022**, *22*, 3765–3785. [CrossRef]
26. Zheng, G.; Mergili, M.; Emmer, A.; Allen, S.; Bao, A.; Guo, H.; Stoffel, M. The 2020 Glacial Lake Outburst Flood at Jinwuco, Tibet: Causes, Impacts, and Implications for Hazard and Risk Assessment. *Cryosphere* **2021**, *15*, 1879–1895. [CrossRef]
27. Duan, H.; Yao, X.; Zhang, Y.; Jin, H.; Wang, Q.; Du, Z.; Hu, J.; Wang, B.; Wang, Q. Lake Volume and Potential Hazards of Moraine-Dammed Glacial Lakes—A Case Study of Bienong Co, Southeastern Tibetan Plateau. *Cryosphere* **2023**, *17*, 591–616. [CrossRef]
28. Mergili, M.; Pudasaini, S.P.; Emmer, A.; Fischer, J.-T.; Cochachin, A.; Frey, H. Reconstruction of the 1941 GLOF Process Chain at Lake Palcacocha (Cordillera Blanca, Peru). *Hydrol. Earth Syst. Sci.* **2020**, *24*, 93–114. [CrossRef]
29. Das, S.; Ramsankaran, R. In-Situ Bathymetry and Volume Estimation of Four Glacial Lakes in Western Himalaya. *J. Glaciol.* **2025**, *71*, e95. [CrossRef]
30. Muñoz, R.; Huggel, C.; Frey, H.; Cochachin, A.; Haeberli, W. Glacial Lake Depth and Volume Estimation Based on a Large Bathymetric Dataset from the Cordillera Blanca, Peru. *Earth Surf. Process. Landf.* **2020**, *45*, 1510–1527. [CrossRef]
31. Zhang, G.; Bolch, T.; Yao, T.; Rounce, D.R.; Chen, W.; Veh, G.; King, O.; Allen, S.K.; Wang, M.; Wang, W. Underestimated Mass Loss from Lake-Terminating Glaciers in the Greater Himalaya. *Nat. Geosci.* **2023**, *16*, 333–338. [CrossRef]
32. Qi, M.; Liu, S.; Wu, K.; Zhu, Y.; Xie, F.; Jin, H.; Gao, Y.; Yao, X. Improving the Accuracy of Glacial Lake Volume Estimation: A Case Study in the Poiqu Basin, Central Himalayas. *J. Hydrol.* **2022**, *610*, 127973. [CrossRef]
33. Lv, J.; Li, S.; Wang, X.; Qi, C.; Zhang, M. Long-Term Satellite-Derived Bathymetry of Arctic Supraglacial Lake from ICESat-2 and Sentinel-2. *Int. Arch. Photogramm. Remote Sens. Spat. Inf. Sci.* **2024**, *XLVIII-1*, 469–477. [CrossRef]
34. Datta, R.T.; Wouters, B. Supraglacial Lake Bathymetry Automatically Derived from ICESat-2 Constraining Lake Depth Estimates from Multi-Source Satellite Imagery. *Cryosphere* **2021**, *15*, 5115–5132. [CrossRef]
35. Fair, Z.; Flanner, M.; Brunt, K.M.; Fricker, H.A.; Gardner, A. Using ICESat-2 and Operation IceBridge Altimetry for Supraglacial Lake Depth Retrievals. *Cryosphere* **2020**, *14*, 4253–4263. [CrossRef]

36. Kalybekova, A. A Review of Advancements and Applications of Satellite-Derived Bathymetry. *Eng. Sci.* **2025**, *35*, 1541. [CrossRef]
37. Armon, M.; Dente, E.; Shmilovitz, Y.; Mushkin, A.; Cohen, T.J.; Morin, E.; Enzel, Y. Determining Bathymetry of Shallow and Ephemeral Desert Lakes Using Satellite Imagery and Altimetry. *Geophys. Res. Lett.* **2020**, *47*, e2020GL087367. [CrossRef]
38. Song, C.; Huang, B.; Ke, L.; Richards, K.S. Remote Sensing of Alpine Lake Water Environment Changes on the Tibetan Plateau and Surroundings: A Review. *ISPRS J. Photogramm. Remote Sens.* **2014**, *92*, 26–37. [CrossRef]
39. Kumar, A.; Mal, S.; Schickhoff, U.; Allen, S.; Dimri, A.P. Assessing the Role of Regional Characteristics in Estimating the Volume of Glacial Lakes in the Upper Indus-Ganga-Brahmaputra Basins, Hindu Kush Himalaya. *J. Hydrol.* **2025**, *657*, 133016. [CrossRef]
40. Kapitsa, V.; Shahgedanova, M.; Kasatkin, N.; Severskiy, I.; Kasenov, M.; Yegorov, A.; Tatkova, M. Bathymetries of Proglacial Lakes: A New Data Set from the Northern Tien Shan, Kazakhstan. *Front. Earth Sci.* **2023**, *11*, 1192719. [CrossRef]
41. Wood, J.L.; Harrison, S.; Wilson, R.; Emmer, A.; Yarleque, C.; Glasser, N.F.; Torres, J.C.; Caballero, A.; Araujo, J.; Bennett, G.L.; et al. Contemporary Glacial Lakes in the Peruvian Andes. *Glob. Planet. Change* **2021**, *204*, 103574. [CrossRef]
42. Watson, C.S.; Quincey, D.J.; Carrivick, J.L.; Smith, M.W.; Rowan, A.V.; Richardson, R. Heterogeneous Water Storage and Thermal Regime of Supraglacial Ponds on Debris-Covered Glaciers. *Earth Surf. Process. Landf.* **2018**, *43*, 229–241. [CrossRef]
43. Kapitsa, V.; Shahgedanova, M.; Machguth, H.; Severskiy, I.; Medeu, A. Assessment of Evolution and Risks of Glacier Lake Outbursts in the Djungarskiy Alatau, Central Asia, Using Landsat Imagery and Glacier Bed Topography Modelling. *Nat. Hazards Earth Syst. Sci.* **2017**, *17*, 1837–1856. [CrossRef]
44. Patel, L.K.; Sharma, P.; Laluraj, C.M.; Thamban, M.; Singh, A.; Ravindra, R. A Geospatial Analysis of Samudra Tapu and Gepang Gath Glacial Lakes in the Chandra Basin, Western Himalaya. *Nat. Hazards* **2017**, *86*, 1275–1290. [CrossRef]
45. Cook, S.J.; Quincey, D.J. Estimating the Volume of Alpine Glacial Lakes. *Earth Surf. Dyn.* **2015**, *3*, 559–575. [CrossRef]
46. Khanal, N.R.; Hu, J.-M.; Mool, P. Glacial Lake Outburst Flood Risk in the Poiqu/Bhote Koshi/Sun Koshi River Basin in the Central Himalayas. *Mt. Res. Dev.* **2015**, *35*, 351–364. [CrossRef]
47. Emmer, A.; Cochachin, A. The Causes and Mechanisms of Moraine-Dammed Lake Failures in the Cordillera Blanca, North American Cordillera, and Himalayas. *AUC Geogr.* **2013**, *48*, 5–15. [CrossRef]
48. Loriaux, T.; Casassa, G. Evolution of Glacial Lakes from the Northern Patagonia Icefield and Terrestrial Water Storage in a Sea-Level Rise Context. *Glob. Planet. Change* **2013**, *102*, 33–40. [CrossRef]
49. Wang, X.; Liu, S.; Ding, Y.; Guo, W.; Jiang, Z.; Lin, J.; Han, Y. An Approach for Estimating the Breach Probabilities of Moraine-Dammed Lakes in the Chinese Himalayas Using Remote-Sensing Data. *Nat. Hazards Earth Syst. Sci.* **2012**, *12*, 3109–3122. [CrossRef]
50. Sakai, A. Glacial Lakes in the Himalayas: A Review on Formation and Expansion Processes. *Glob. Environ. Res.* **2012**, *16*, 23–30. [CrossRef]
51. Huggel, C.; Kääb, A.; Haeberli, W.; Teysseire, P.; Paul, F. Remote Sensing Based Assessment of Hazards from Glacier Lake Outbursts: A Case Study in the Swiss Alps. *Can. Geotech. J.* **2002**, *39*, 316–330. [CrossRef]
52. Evans, S.G. Landslide Damming in the Cordillera of Western Canada. In *Landslide Dams: Processes, Risk, and Mitigation*; ASCE: Reston, VA, USA, 1986; pp. 111–130.
53. Wilson, R.; Glasser, N.F.; Reynolds, J.M.; Harrison, S.; Anacona, P.I.; Schaefer, M.; Shannon, S. Glacial Lakes of the Central and Patagonian Andes. *Glob. Planet. Change* **2018**, *162*, 275–291. [CrossRef]
54. Huggel, C.; Haeberli, W.; Kääb, A.; Bieri, D.; Richardson, S. An Assessment Procedure for Glacial Hazards in the Swiss Alps. *Can. Geotech. J.* **2004**, *41*, 1068–1083. [CrossRef]
55. Wei, J.; Liu, S.; Wang, X.; Zhang, Y.; Jiang, Z.; Wu, K.; Zhang, Z.; Zhang, T. Longbasaba Glacier Recession and Contribution to Its Proglacial Lake Volume between 1988 and 2018. *J. Glaciol.* **2021**, *67*, 473–484. [CrossRef]
56. King, O.; Dehecq, A.; Quincey, D.; Carrivick, J. Contrasting Geometric and Dynamic Evolution of Lake and Land-Terminating Glaciers in the Central Himalaya. *Glob. Planet. Change* **2018**, *167*, 46–60. [CrossRef]
57. Zhang, T.; Wang, W.; An, B. A Conceptual Model for Glacial Lake Bathymetric Distribution. *Cryosphere* **2023**, *17*, 5137–5154. [CrossRef]
58. Wang, J.; Wu, F.; Zhang, J.; Khanal, G.; Yang, L. The Himalayan Collisional Orogeny: A Metamorphic Perspective. *Acta Geol. Sin.-Engl. Ed.* **2022**, *96*, 1842–1866. [CrossRef]
59. Nie, Y.; Pritchard, H.D.; Liu, Q.; Hennig, T.; Wang, W.; Wang, X.; Liu, S.; Nepal, S.; Samyn, D.; Hewitt, K.; et al. Glacial Change and Hydrological Implications in the Himalaya and Karakoram. *Nat. Rev. Earth Environ.* **2021**, *2*, 91–106. [CrossRef]
60. Wang, Y.; Yang, K.; Zhou, X.; Wang, B.; Chen, D.; Lu, H.; Lin, C.; Zhang, F. The Formation of a Dry-belt in the North Side of Central Himalaya Mountains. *Geophys. Res. Lett.* **2019**, *46*, 2993–3000. [CrossRef]
61. Bookhagen, B.; Burbank, D.W. Toward a Complete Himalayan Hydrological Budget: Spatiotemporal Distribution of Snowmelt and Rainfall and Their Impact on River Discharge. *J. Geophys. Res. Earth Surf.* **2010**, *115*, F3. [CrossRef]
62. Wang, X.; Pang, G.; Yang, M. Precipitation over the Tibetan Plateau during Recent Decades: A Review Based on Observations and Simulations. *Int. J. Climatol.* **2018**, *38*, 1116–1131. [CrossRef]

63. Zhang, J.; You, Q.; Wu, F.; Cai, Z.; Pepin, N. The Warming of the Tibetan Plateau in Response to Transient and Stabilized 2.0 °C/1.5 °C Global Warming Targets. *Adv. Atmos. Sci.* **2022**, *39*, 1198–1206. [CrossRef]
64. You, Q.; Chen, D.; Wu, F.; Pepin, N.; Cai, Z.; Ahrens, B.; Jiang, Z.; Wu, Z.; Kang, S.; AghaKouchak, A. Elevation Dependent Warming over the Tibetan Plateau: Patterns, Mechanisms and Perspectives. *Earth-Sci. Rev.* **2020**, *210*, 103349. [CrossRef]
65. Krishnan, R.; Shrestha, A.B.; Ren, G.; Rajbhandari, R.; Saeed, S.; Sanjay, J.; Syed, A.; Vellore, R.; Xu, Y.; You, Q.; et al. Unravelling Climate Change in the Hindu Kush Himalaya: Rapid Warming in the Mountains and Increasing Extremes. In *The Hindu Kush Himalaya Assessment: Mountains, Climate Change, Sustainability and People*; Springer International Publishing: Cham, Switzerland, 2019; pp. 57–97. [CrossRef]
66. Yin, A. Cenozoic Tectonic Evolution of the Himalayan Orogen as Constrained by Along-Strike Variation of Structural Geometry, Exhumation History, and Foreland Sedimentation. *Earth-Sci. Rev.* **2006**, *76*, 1–131. [CrossRef]
67. Ding, L.; Spicer, R.A.; Yang, J.; Xu, Q.; Cai, F.; Li, S.; Lai, Q.; Wang, H.; Spicer, T.E.V.; Yue, Y.; et al. Quantifying the Rise of the Himalaya Orogen and Implications for the South Asian Monsoon. *Geology* **2017**, *45*, 215–218. [CrossRef]
68. Clift, P.D.; Giosan, L.; Blusztajn, J.; Campbell, I.H.; Allen, C.; Pringle, M.; Tabrez, A.R.; Danish, M.; Rabbani, M.M.; Alizai, A.; et al. Holocene Erosion of the Lesser Himalaya Triggered by Intensified Summer Monsoon. *Geology* **2008**, *36*, 79. [CrossRef]
69. Liu, S.; Yao, X.; Guo, W.; Xu, J.; Shangguan, D.; Wei, J.; Bao, W.; Wu, L. The Contemporary Glaciers in China Based on the Second Chinese Glacier Inventory. *Acta Geogr. Sin.* **2015**, *70*, 3–16. [CrossRef]
70. Veh, G.; Korup, O.; Von Specht, S.; Roessner, S.; Walz, A. Unchanged Frequency of Moraine-Dammed Glacial Lake Outburst Floods in the Himalaya. *Nat. Clim. Change* **2019**, *9*, 379–383. [CrossRef]
71. Harrison, S.; Kargel, J.S.; Huggel, C.; Reynolds, J.; Shugar, D.H.; Betts, R.A.; Emmer, A.; Glasser, N.; Haritashya, U.K.; Klimeš, J.; et al. Climate Change and the Global Pattern of Moraine-Dammed Glacial Lake Outburst Floods. *Cryosphere* **2018**, *12*, 1195–1209. [CrossRef]
72. Fujita, K.; Sakai, A.; Takenaka, S.; Nuimura, T.; Surazakov, A.B.; Sawagaki, T.; Yamanokuchi, T. Potential Flood Volume of Himalayan Glacial Lakes. *Nat. Hazards Earth Syst. Sci.* **2013**, *13*, 1827–1839. [CrossRef]
73. Popov, N.V. Assessment of Glacial Debris Flow Hazard in the North Tien-Shan. In *Proceedings of the Soviet-China-JapanSymposium and Field Workshop on Natural Disasters*; USSR: Urumgi, China, 1991; pp. 384–391.
74. Emmer, A.; Vilímek, V. Review Article: Lake and Breach Hazard Assessment for Moraine-Dammed Lakes: An Example from the Cordillera Blanca (Peru). *Nat. Hazards Earth Syst. Sci.* **2013**, *13*, 1551–1565. [CrossRef]
75. Hardmeier, F.; Schmidheiny, N.; Suremann, J.; Lüthi, M.; Vieli, A. Evolution, Sedimentation and Thermal State of the Emerging pro-Glacial Lakes at Witenwasserengletscher, Switzerland. *Earth Surf. Process. Landf.* **2024**, *49*, 4055–4073. [CrossRef]
76. Bazai, N.A.; Carling, P.A.; Cui, P.; Hao, W.; Guotao, Z.; Dingzhu, L.; Hassan, J. Refining Lake Volume Estimation and Critical Depth Identification for Enhanced Glacial Lake Outburst Flood (GLOF) Event Anticipation. *Cryosphere* **2024**, *18*, 5921–5938. [CrossRef]
77. Steffen, T.; Huss, M.; Estermann, R.; Hodel, E.; Farinotti, D. Volume, Evolution, and Sedimentation of Future Glacier Lakes in Switzerland over the 21st Century. *Earth Surf. Dyn.* **2022**, *10*, 723–741. [CrossRef]